SCIENTIFIC REPORTS

On the Stability and Abundance of Single Walled Carbon Nanotubes

Daniel Hedman[1,*], Hamid Reza Barzegar[2,4,*], Arne Rosén[3], Thomas Wågberg[2] & J. Andreas Larsson[1]

Many nanotechnological applications, using single-walled carbon nanotubes (SWNTs), are only possible with a uniform product. Thus, direct control over the product during chemical vapor deposition (CVD) growth of SWNT is desirable, and much effort has been made towards the ultimate goal of chirality-controlled growth of SWNTs. We have used density functional theory (DFT) to compute the stability of SWNT fragments of all chiralities in the series representing the targeted products for such applications, which we compare to the chiralities of the actual CVD products from all properly analyzed experiments. From this comparison we find that in 84% of the cases the experimental product represents chiralities among the most stable SWNT fragments (within 0.2 eV) from the computations. Our analysis shows that the diameter of the SWNT product is governed by the well-known relation to size of the catalytic nanoparticles, and the specific chirality is normally determined by the product's relative stability, suggesting thermodynamic control at the early stage of product formation. Based on our findings, we discuss the effect of other experimental parameters on the chirality of the product. Furthermore, we highlight the possibility to produce any tube chirality in the context of recent published work on seeded-controlled growth.

Single-walled carbon nanotubes (SWNTs) possess remarkable electrical, mechanical and chemical properties, and are widely discussed for various applications such as integration in electronic circuits[1–3], mechanical reinforcement of light-weight composites[4,5], as well as for chemical- and bio-sensors[6,7] and synthetic muscles[8]. However, many applications rely on having SWNTs with defined properties and, since both electrical and structural characteristics of SWNTs can vary greatly depending on the chirality and diameter, huge efforts have been made to either selectively grow SWNT with single or few chiralities[9–21] or to post-purify them after synthesis[22–31]. Alternatively, efforts have been made to tailor SWNT properties by chemical doping[32–42], which significantly affects the electrical and chemical properties of SWNTs.

Although the post-purification methods result in relatively high yield of certain chiralities; such methods are expensive and time consuming, and may modify the properties of the tube, for example, by functionalization or structural damage. The chemical doping approach, on the other hand, suffers from the fact that the dopant elements can incorporate into SWNTs in different configurations; therefore doped samples are usually inhomogeneous. The limitations and disadvantages of the post modification methods have encouraged researchers to continue investigating possible approaches to selectively grow SWNTs. Chemical vapor deposition (CVD) has become the most promising technique for this purpose, since it involves several controllable growth parameters. The vapor-liquid-solid[43–45] (VLS) mechanism of fiber growth serves as a basis for understanding SWNT growth through catalytic-CVD, but one also has to account for the tubes being hollow: Since this results in an unstable growing end that has to be stabilized by a catalyst particle that has the metal–carbon binding energy in the required region–not too weak and not too strong, following a "Goldilocks" principle that is only fulfilled for a limited number of

[1]Applied Physics, Division of Materials Science, Department of Engineering Sciences and Mathematics, Luleå University of Technology, SE-971 87 Luleå, Sweden. [2]Department of Physics, Umeå University, SE-901 87 Umeå, Sweden. [3]Department of Physics, University of Gothenburg, SE-412 96 Göteborg, Sweden. [4]Department of Physics, University of California and the Lawrence Berkeley National Laboratory, Berkeley CA 94720, USA. *These authors contribed equally to this work. Correspondence and requests for materials should be addressed to J.A.L. (email: andreas.1.larsson@ltu.se)

metals[46–49], and can be tuned by alloying[50,51]. It has been shown that it is possible to affect the chirality of the growing SWNT by varying the experimental conditions, such as catalyst composition[12,14–16,52–55] temperature[56], carbon precursor[10,17], carrier gas pressure[57], and catalyst support[11,18]. Concurrently, several reports have investigated the energetic stability of different chiralities[58,59] and their caps[60–63], and some studies have also compared theoretical and experimental data in an effort to clarify the production of SWNTs of certain chiralities[64,65]. However, despite numerous studies on the production of SWNTs, a detailed understanding of the correlation between experiment and theory is lacking. In our study we try to answer the following key questions; i) To what extent can the observed statistical abundance of certain SWNT chiralities be explained by their energetic stability?, ii) What experimental growth parameters have high impact on the chirality of the growing SWNT?, iii) Why are certain tubes so seldom observed in experimental studies? and, finally, iv) What strategy should be followed to obtain a high relative abundance of more exotic tubes seldom seen in SWNT products?

We try to answer these questions by taking advantage of all relevant experimental studies made so far, meaning that we consider experiments where methods have been used that are able to properly detect all or nearly all present SWNT chiralities in a sample with tolerable statistics. SWNTs with different chiralities and diameters all have unique band structures, which influences the criteria for eligible detection techniques. For example, photo-luminescence only detects semiconductor SWNTs and in the case of Raman spectroscopy it is necessary to have excitation wavelengths equal to the difference between van Hove singularity (VHS) pairs to satisfy the resonance condition[66–68]. In the literature survey made for our comparison of theoretical stability and experimental abundance we have defined three main techniques that we deem to be appropriate to meet this criterion; either a combination of photo-luminescence, electron diffraction, and/or ultraviolet-visible-near infrared spectroscopy or Raman spectroscopy obtained by at least three different excitation lasers evenly distributed over the wavelength region from 450–1054 nm (1.2–2.8 eV). A single study that utilizes surface enhanced Raman spectroscopy is also considered in the study, as it seems to properly detect all present SWNTs[69]. There is a risk that even in the selected studies some tubes might be out of resonance with the excitation wavelength used for detection, but since our statistics are based on number of "hits" and not the statistical abundance, and since each resonance window for a SWNT is roughly 0.3 eV[70], we believe that our criterion gives valid data for our analysis. The data from the experimental studies are collected in Table S1 in the supplementary material. The combined experimental data are discussed in the context of theoretical data on the energetic stability of eleven different SWNT-series, namely the (n + m = 8) to (n + m = 18) series, where n and m are the SWNT chiral indices.

Methods

We have calculated the total energy of all carbon nanotube series for which $(n + m) = 8, 9, 10, ..., 18$ using density functional theory (DFT). The nanotubes were modeled using six-layered hydrogen terminated structures, for which the number of carbon atoms per layer is equal to $2(n + m)$ (see inset to Fig. 1). These structures were placed in a $27 \times 27 \times 27$ Å cubic box, giving at least 10 Å of vacuum separation between the periodic images.

The DFT calculations were performed using the Vienna Ab initio Simulation Package[71] (VASP). Only the gamma point was used in the calculations to minimize the interactions between periodic images. The calculations were performed using the projector-augmented wave method[72], a plane wave basis set and the Perdew-Burke-Ernzerhof (PBE) exchange-correlation functional[73]. The plane wave basis set energy cutoff was set to 575 eV and the electronic self-consistence loop was converged to 1×10^{-6} eV.

Gaussian smearing was used; the smearing width (SIGMA) was adjusted in order to give energies associated with the electronic entropy of approximately 0.5 meV/atom. All of the calculations were spin polarized (ISPIN = 2), with an antiferromagnetic initial magnetization (one end of the SWNT spin up and the other spin down). The nanotube structures were relaxed with no symmetry constraints using the conjugate-gradient algorithm, until all of the forces acting on the ions were smaller than 6×10^{-3} eV/Å.

The formation enthalpy H_f was calculated using a simplified version of the equation given in[74]

$$H_f = E(n, m) - a \cdot E_C - \frac{b \cdot E_H}{2}$$

(1)

Here, $E(n,m)$ is the energy of the SWNT, $E_C = -9.201514$ eV is the energy per C atom for a 500 atom super-cell of graphite and $E_H = -6.771933$ eV is the energy for an H_2 molecule in a $27 \times 27 \times 27$ Å cubic box. $a = 6 \times 2(n + m)$ is equal to the number of carbon atoms in the nanotube and $b = 2(n + m)$ is the number of hydrogen atoms used for termination of the nanotube ends. The diameters of the SWNTs were determined using the relaxed structures through the radial distance to the center-line of the tube averaged over the 4 central layers (excluding the hydrogen atoms and one layer at each side of the tube).

Results and Discussion

We have computed the total energies of six-layer SWNT segments of the (n + m = 8) to (n + m = 18) series with hydrogen-terminated ends (see inset to Fig. 1). The relative energies of the segments within each series are shown in Fig. 1, meaning that the most stable tube in each series corresponds to zero energy. As reported in earlier studies, hydrogen-terminated tube segments with a zigzag character have
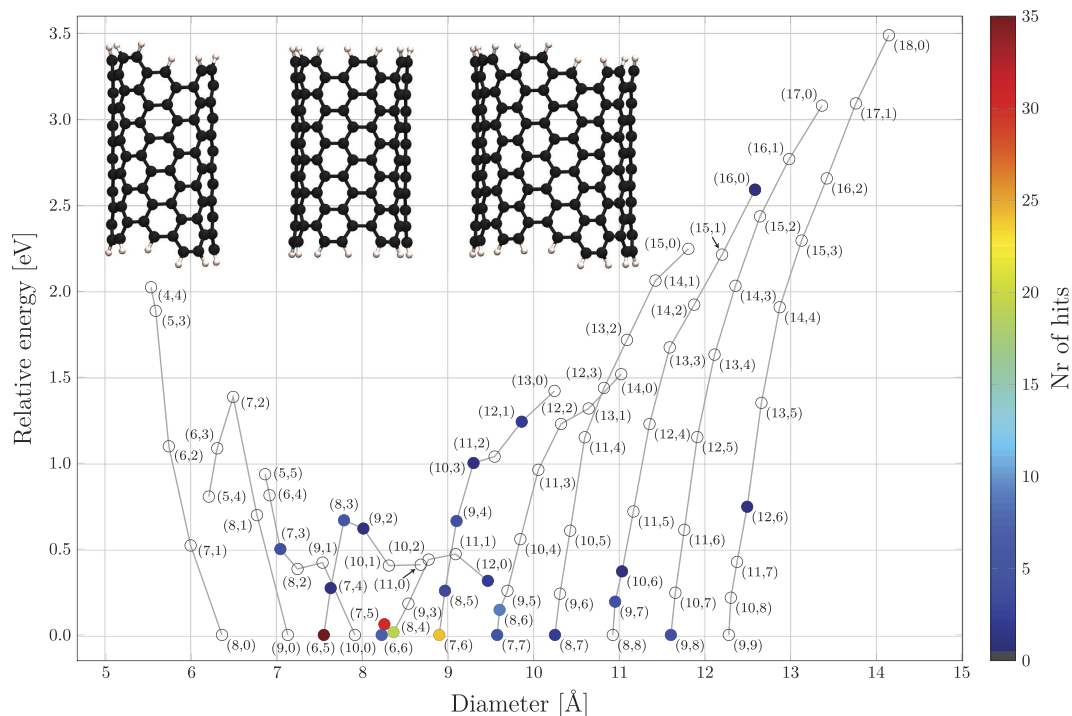
Figure 1. Relative energies between SWNTs of each (n + m) series from (n + m) = 8 to 18 plotted against the nanotube segment diameter. The zero line thus represents the most stable tube in each series. The colored points represent products from SWNT growth, with the color code representing the hit-rate of how many times a particular SWNT has been reported as a product in a unique CVD experiment (see Table S1). Inset shows the hydrogen terminated six-layer SWNT segments of the (6,5), (6,6) and (9,8) armchair and near-armchair tubes.

| Series	8	9	10	11	12	13	14	15	16	17	18
ΔE (eV)	2.023	1.385	0.935	0.667	0.470	1.420	1.517	2.246	2.590	3.079	3.489

Table 1. Energy windows (ΔE) of the difference between the most stable and least stable SWNT within the series.

antiferromagnetic ground states[75–77]. We report energy windows (ΔE) of the difference between the most stable and least stable SWNT within the series (see Table 1) in agreement with previously reported values for the 9 to 11 series[58], and the 12 and 13 series[59].

In the lower series 8 to 10 zigzag tubes are the most stable while in the other series (11 to 18) armchair tubes are the most stable. In the 13-series and above the stability follows the chiral index, with the zigzag tubes being the least stable within each series. In the 8 series the stability follows the reverse order, with the armchair tube being the least stable. In the 9 series the order of stability is (9, 0), (8, 1), (5, 4), (6, 3), and (7, 2). In the 10 series the order is (10, 0), (8, 2), (9, 1), (7, 3), (6, 4), and (5, 5), and in the 11-series it is (6, 5), (7, 4), (10, 1) and (11, 0) only differing with 5 meV, (9, 2) and (8, 3). In the 12-series the order is (6, 6), (8, 4), (7, 5), (9, 3) (12, 0), (10, 2) and (11, 1).

We have reviewed the reported SWNTs in all relevant experimental studies[10–12,14–18,20,21,52–57,69,78–89], which properly detect all present SWNT chiralities in the sample, and correlate the resulting statistics with the computed relative stabilities in Fig. 1. Specific CVD conditions are tabulated in Table S1 in the supplementary material.

Four observations can be made from this rather simplistic experimental/theoretical comparison: Firstly, there are no reported SWNT products in the 8 and 9 series (and only (7,3) from the 10 series), which we attribute to the fact that these small-diameter tubes have formation enthalpies that are too large (see Fig. 2). Secondly, most of the products are in the 10 to 14 series, although the formation enthalpies of the higher series are progressively lower. We argue that this is the result of the catalyst particle size targeted in the majority of these studies, as there is plenty of evidence for the relationship between catalytic metal nanoparticle size and the diameter of the grown tubes[20,86,90,91]. Thirdly, and most importantly,
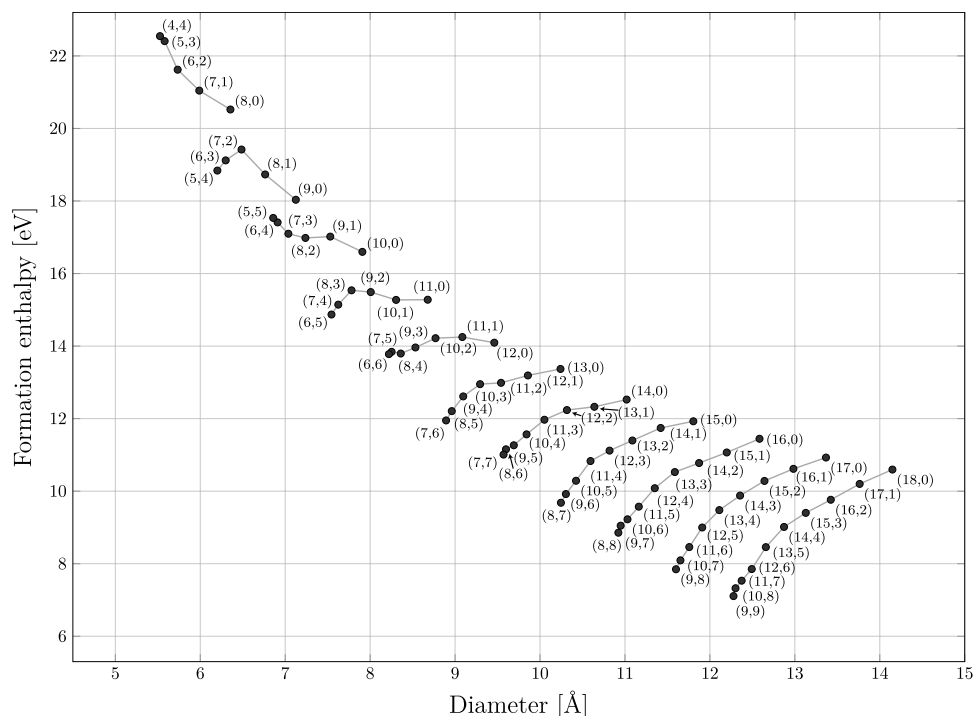
Figure 2. Formation enthalpy of each SWNT in this study (as defined by Eq. (1) in the main text) plotted against the nanotube segment diameter. This figure thus displays the energies of the tubes on a comparable scale.

we observe that the vast majority of all SWNT products found in the experimental reports are among the most stable tubes in its series. This is a very surprising finding, since the energy differences between different chiralities are rather small, especially considering the differences in stability between the different series (see the formation enthalpies in Fig. 2)[92,93]. We have thus found that if no special measures are taken, the majority of the grown SWNTs will correspond to the few most stable SWNTs within the series, under the condition that the nanotube diameter matches the size of the metal nanoparticles used to catalyze the growth of the SWNT. Fourthly, we note, however, that there seems to be one major exception to the strong correlation between abundance and energetic stability; All experimental data indicate significantly lower abundance of pure armchair tubes (n=m) compared to near-armchair tubes (n≈m), despite the fact that armchair tubes display higher energetic stability, especially for series 12 and higher (see values for (6,6), (7,7), (8,8) and (9,9) in Fig. 1). The explanation for this can be found in the work by Yakobson group, who report that pure-armchair tubes (and pure-zigzag tubes) grow by a different growth mechanism than all other (so-called chiral) tubes that grow from screw-dislocations[64,65]. As a result, armchair and zigzag tubes will grow significantly more slowly (and hence be shorter) than chiral tubes. Since spectroscopic techniques such as Raman spectroscopy and photoluminescence scale with number of phonons, and number of electrons in the VHS, respectively, they both scale with number of atoms in the SWNTs, and hence an equal abundance of e.g. the armchair (6,6) and the chiral (7,5) tube in a given experiment will display a weaker signal of the armchair tube, since these have a shorter length[94]. It is important to point out that this observation does not rule out the possibility to target pure-armchair tubes as the main product, as recently shown by Sanchez-Valencia et al.[89], since when using synthesized molecules as seeds (as discussed later) such tubes can indeed dominate. We note that our computational data points toward the (10,0) zigzag tube being produced in CVD growth using small diameter catalytic particles, but their short lengths make them undetectable.

We have found that the majority (84%) of the experimental product (hit-rate in Fig. 1) is among the most stable SWNT fragments (below 0.2 eV). Looking at tubes with similar diameter it is clear that, in addition to the relative energies of the tubes within the same series, the differences in formation enthalpy (see Fig. 2) is essential in understanding what SWNTs are formed: Clear examples where the formation enthalpy plays a major role in the growth abundance of certain chiralities can be seen by comparing e.g., the (7,5) and (8,4) tubes of the 12 series that both have significantly higher "hit-rates" than the (10,1) tube of the 11 series that have similar diameter as the (7,5) and the (8,4) tubes but a formation enthalpy that is around 2 eV higher. Similar observations can be made for the abundant (7,7) and (8,6) tubes of the 14 series and the rarely seen (10,3) and (11,2) tubes of the 13 series with similar diameters but much higher formation enthalpy. The above analysis of the data in Fig. 2 shows comprehensively how the
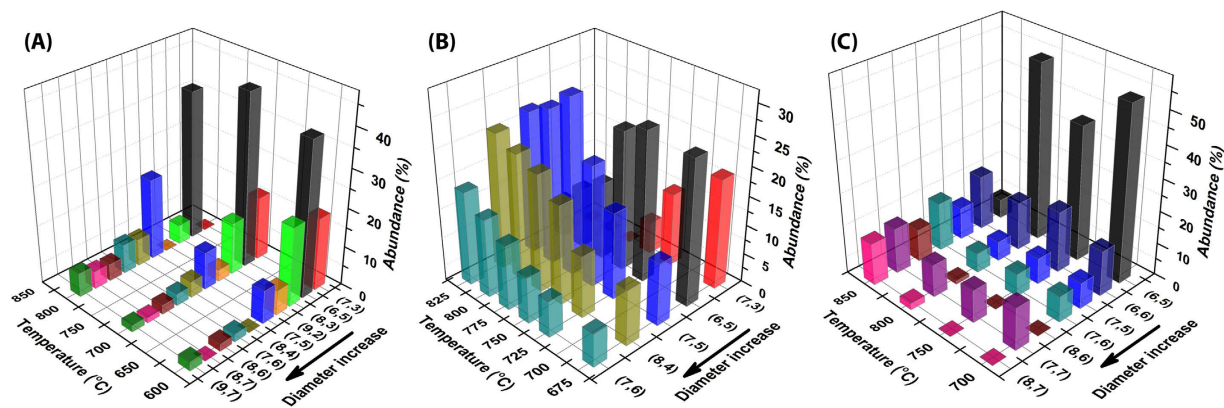
Figure 3. Effect of temperature on chirality distribution (**a**) represented from work by Loebick *et al.*[86] (**b**) represented from work by Wei *et al.*[85] (**c**) represented from work by Lolli *et al.*[56]. The arrows indicate the direction of diameter increase.

experimental hits are concentrated near the baseline when recasting the data into series disregarding the stability relation between different series, as in Fig. 1. Lastly, we want to point out the rather remarkable fact that we have been able to draw all these conclusions using just SWNT segments, *without considering* their interface with the catalytic metal.

Growth parameters discussion. In the context of our findings that the catalyst particle size together with the relative energetic stability represent the two most important criteria that influence the growth of specific SWNT chiralities, we review the effects of the other growth parameters, temperature, pressure, feedstock, substrate and catalyst composition, on the selective growth of SWNTs.

Temperature. The most distinct impact that temperature has on the growth products is the increase in overall tube diameters. This is obvious from Fig. 3a–c. The increase in diameter can be rationalized by an effect on the catalytic metal nanoparticles known as Ostwald ripening[95–98] at temperatures above 700 °C, meaning that the metal atoms become more mobile when the temperature rises. The result is disappearance of small metal nanoparticles where the material builds up the size of the remaining particles, as well as other temperature effects, such as agglomeration. This is exemplified by the report by Loebick *et al.*[86], who showed that the average size of Co nanoparticles increases with temperature in the CVD reaction chamber. Although, in their work, the Co nanoparticles were deposited on MCM-41 mesoporous silica template and mixed with Mn to minimize the effect of temperature, still, the average diameter of the catalyst particles increases slightly at higher temperature, namely from 8 Å at 600 °C to 12.5 Å at 800 °C (at intermediate temperature, 700 °C, the particle size increases to 9 Å). As a result, the dominating SWNTs in the sample are also shifted, as represented in Fig. 3a, showing the chirality distribution *vs* growth temperature. Further, it is interesting to note that production of tubes with high relative energy for the diameters represented by the metal particle size distribution in this specific experiment, such as the (7,3), (8,3) and (9,2), is shifted to production of tubes with lower relative energy such as (8,4), (8,6), and (9,7) (*cf.* Fig. 1). This phenomenon will be further discussed below. The change in particle size (tube diameter) with temperature seems to be more significant in smooth (nonporous, weakly interacting) substrates such as silicon wafer. For instance, Fouquet *et al.*[14] observed an up-shift in diameter distribution of the grown SWNT from 6.1–11.9 Å for 600 °C (growth temperature) to 6.3–14.9 Å for 700 °C, for Co catalyst deposited on a silicon wafer. The temperature increase also shifts the dominant chiralities from (6,5), (6,6) and (7,4) for 600 °C to (7,5), (7,6) and (10,9) tube for 700 °C. These observations manifest our previous statement about the strong correlation between relative energetic stability and high abundance under the pre-requirement of matching catalyst particle size since, although these tubes belong to different series with different formation enthalpies (see Fig. 2), the "new" observed tubes also have the lowest energies in each series but with larger diameters (see Fig. 1). Figure 3b,c show two other examples of the temperature effect: Wei *et al.*[85] grew SWNTs by plasma-enhanced ethanol decomposition using Co catalyst particles supported on MCM41, while Lolli *et al.*[56] studied the temperature effect for SWNT growth on CoMo catalysts. In our report we have given a few representative examples to reveal the effect of temperature on the selective growth process by highlighting studies that have examined the chirality distribution in detail. Our conclusions are, however, perfectly valid when compared with the data in other work[16,80–82].

Pressure. We also consider the carbon precursor pressure in the reaction chamber, which has been shown to have a significant effect on the chirality distribution. The influence of this parameter is, however,

more complex to study, since it may also relate to the composition of the catalyst particles, with regard to their carbon saturation, especially at elevated temperature. Picher et al.[99] showed that a combination of precursor pressure and reaction temperature affects the chirality distribution of the growing SWNTs and suggest that, compared to large catalyst particles, small catalyst particles can withstand higher carbon content before saturation. As a consequence, at a specific temperature, higher carbon precursor pressure will result in preferential activation of small catalyst particles and, consequently, preferential growth of small diameter tubes. A similar conclusion was made by Wang et al.[57], who studied carbon precursor pressure ranging from 2 to 18 bar at fixed reaction temperature.

Feedstock. Figure. 3a,b also introduce another important parameter for SWNT growth: the choice of carbon precursor. While Loebick et al.[86] used CO (Fig. 3a) as carbon precursor, Wei et al.[85] used ethanol. Several studies have speculated that the hydrogen produced when using a hydrocarbon as precursor affects the rate of catalyst particle reduction, remaining active for a longer time[56,100,101]. This is consistent with the results presented in Fig. 3a,b, showing a distribution with more small-diameter tubes for the CO precursor. Similar results have also been observed in other reports[99]. Wang et al.[10], examined four different carbon precursors; CO, C_2H_2, C_2H_5OH and CH_3OH to grow SWNTs and they also observed a clear shift to large-diameter tubes when hydrocarbons were used compared to CO.

Substrate. The studies presented in Fig. 3a,b utilize CoMn and Co catalyst particles deposited on MCM41. Here, it is interesting to note that Mn is highly stable against reduction and does not act as a catalyst for SWNT growth (too large M-C bond strength)[49], but instead acts in the alloy to prevent melting and evaporation of Co from the particles, thereby minimizing the effect of Ostwald ripening and agglomeration. This is the reason that the chirality distribution is less affected by temperature in Fig. 3a. For the same reason, inclusion of other non-catalytic metals (e.g., Mo, W, Cr, etc.) into the catalytic particles has a positive effect, producing uniform distributions of SWNTs, most likely because they help to reduce the effect of temperature[10,19,55]. It should be noted that inclusion of these metals also affects the catalytic particles' effective M-C bond strength[50,51]. We also find that at low temperature these alloy catalysts lead to production of tubes with higher relative energy for the diameters represented by the metal particle size distribution in this specific experiment ((7,3), (8,3) and (9,2) in Fig. 3a). The reason for this is that the surface geometry of the particles does not adapt, but remains frozen (see more about this effect below). These observations also relate to the very important relation between the catalyst particles and the substrates for SWNT growth. Such particle-substrate interaction can also prevent restructuring of the particles driven by temperature as well as affecting the morphology of catalyst particles. Lolli et al.[56] used CoMo supported on two different materials, SiO_2 and MgO, to grow SWNTs under similar reaction conditions. Interestingly, the chirality distribution was broader when MgO was used as support, which the authors explain by a difference in particle-substrate interaction as well as a change in the catalyst particle morphology. Thus, the choice of substrate can have an effect on the restructuring of the catalytic particles similar to that of the alloying elements Mn, Mo, W and Cr, which will be considered below.

Catalyst composition. Another parameter that affects the chirality distribution is the interaction between catalyst particle and the dissociating carbon atoms. Within the M-C bond strength "Goldilocks" window of catalytic activity[46–49] (see Introduction), the use of different metals with different bond strengths affects the distribution of SWNT product. This effect has been described by Barzegar et al.[20], who show that slight changes in the Co/Fe ratio of the catalyst particles could influence the chirality distribution. Similarly, H. Chiang et al.[53] observed a change in chirality distribution of the grown SWNTs when they systematically studied a change in catalyst particle composition from pure Fe to pure Ni (with a number of steps utilizing different admixtures of Fe and Ni), while the average catalyst particle size was kept constant.

Overall the experimental and theoretical data strongly suggest that a selective growth mechanism is dictated by a *two-parameter model* in which the *diameter* of the tubes produced is primarily governed by the nature of the catalyst particle, in particular size, and the *specific chirality* is governed by the relative energetic stability at the diameter in question, pointing towards a high degree of thermodynamic control at the initial stage of growth. There are a few exceptions to the two-parameter model. In some cases a relatively high abundance of tubes with lower stability, such as the (7,3), (8,3), (9,2), and the (9,4) tubes, can be found. We have described above that in such cases the conditions to grow "low-stability" tubes occur for SWNT growth at low temperatures. It is reasonable to think that certain metal nanoparticles with ideal size and surface morphology can catalyze the growth of such tubes and that the low temperature hinders adaptation of the nanoparticles to the geometry demanded for more stable tubes with this diameter.

Seeded growth. We subsequently turn our focus to special measures that can be taken in order to promote the growth of energetically unfavorable SWNTs found higher up in the ladder of a series. Two recent reports with very different seeding approaches give important insight into this matter: Sanchez-Valencia et al.[89] use pre-grown chemically synthesized precursors of (6,6) caped segments as seeds to promote the growth of single chirality SWNTs samples. This work is in some aspects inspired by the work by Smalley et al.[102], who use pre-cut SWNT segments as seeds to promote single chirality

growth; Yang *et al.*[69,103], on the other hand, take in two different studies advantage of a metal catalyst with a very high melting temperature, W_6Co_7. By growing nanotubes at 1030 °C a nearly complete selective growth process is achieved, with a 94% selectivity for the (12,6) tube, and a 80% selectivity for the (16,0) tube, respectively. Looking at Fig. 1, it is clear that the (12,6) tube is far from being the most stable tube in the 18 series. The authors explain the stabilization of this specific tube with the very high melting temperature of W_6Co_7 (2500 °C), which results in an unchanged morphology of the faceted catalyst nanoparticles during the CVD growth. The authors also indicate that, under slightly different conditions, other SWNTs with high relative energy for their diameter (as found in the present study, see Fig. 1) can grow, such as (14,4). The hypothesis made by the authors about frozen catalyst surfaces giving preference to certain tubes is fully supported by our observations. Tubes with high relative energy can grow from catalyst nanoparticles that exactly meet the requirement of only this specific chirality when frozen. If the conditions allow, the catalyst nanoparticle will adapt to the shape (and size) that better match the tubes with higher stability, but at low temperature (as discussed previously), for very stable catalyst particles (for example, due to high melting temperature), or for catalyst nanoparticles that are stabilized due to other reasons, exotic low-stability tubes with certain chirality can grow. The latter proposal is supported by our analysis of the experimental data, summarized in Fig. 1, which for some reports indicate a rather high abundance of e.g., the (7,4), (9,2) and (8,3) tubes of the 11 series, and the (8,5), (9,4) and (10,3) tubes of the 13 series. Looking further in Table S1, it can be seen that, in all of these experiments, the catalytic metal particles are deposited on a porous substrate that forms strong bonds to the metal catalyst. We believe that using such substrates results in a broader catalyst particle distribution and that the strong bonds between the particles and the substrate inhibit both reshaping of metal nanoparticles as well as diffusion of metal atoms, resulting in larger particles, thus providing a template for less stable tubes to be formed. The molecular seeds used in the Sanchez-Valencia *et al.*[89] study, on the other hand, represent a very promising development where cap, ring and belt-shaped molecules from chemical synthesis (such as the molecules in ref. 104) could be used to promote the growth of particular SWNTs in a controlled way (as also suggested in ref. 73). Such seeds could also be substrate bound (non-catalytic) with subsequent deposition of the catalyst metal in order to reap the benefits of tip growth, both for feedstock access (SWNT length) and closely packed seeds (SWNT packing density). Bear in mind that the tube with the highest formation enthalpy seen in CVD is the (7,3) tube and, thus, *all tubes with lower formation enthalpy* (*see* Fig. 2) *could be possible products* that could be targeted through seeded growth. The molecular seeding approach can also be used to eliminate the complication of using metal nanoparticles and the tube diameter dependence on their size, since the (6,6) tube growth in ref. [89] was catalyzed by a smooth Pt surface.

We believe that the major effect of the growth temperature, of larger metal particles leading to larger diameter tubes, could just as well be achieved by a pre-treatment annealing of the catalyst with growth at a lower temperature. Furthermore, we suggest that a combination of low temperature and high precursor pressure would result in the smallest diameter tubes. A combination of alloying with Mn, Mo, W, or Cr and/ or a porous and sticky substrate would possibly open up for the production of exotic small diameter tubes.

Conclusions

We have compared computed SWNT fragment stabilities from DFT with all CVD growth experiments evaluated by methods that properly detect all present nanotube chiralities. We have found that the very smallest diameter tubes of the 8, 9, and 10 series are not produced because of high formation enthalpies, but that otherwise the SWNT diameter is governed by the well-known dependence with the catalytic particle size, not by the SWNT formation enthalpy, the latter favoring large-diameter SWNTs. It is, however, natural that tubes of larger diameter than the catalytic particles are not formed. Our most important finding is that the specific chirality of the SWNT product is strongly dependent on the relative stability of the tubes within their series, which can be rationalized to a dependence on the formation enthalpy of tubes of similar diameter. Thus, the dominating SWNT products are among the few most stable in each series, and our study shows that 84% of the products in all reported CVD growth to date is within 0.2 eV of the most stable tube of its series. We wish to point out that our strong correlation between energetic stability and abundance in experimental studies is obtained by only considering the SWNT segments, without the inclusion of the interface with the catalytic metal. We thus conclude that the effect of the actual growth conditions and the interaction with the metal is less dominant with respect to the product outcome, and that the initial formation of the product is governed mainly by thermodynamic control. Regarding the possibility to influence product outcome by fine-tuning the experimental conditions, our analysis shows that the growth temperature has by far the largest effect on the index of the SWNT product. We show, however, that this is directly related to the temperature influence on the metal particle size. At low growth temperatures (below 650 °C), or high melting temperature of the catalyst due to alloying, or strong substrate binding, the "frozen" metal surfaces can act as templates for growth of less stable tubes. Such conditions account for most of the remaining 16% experimental products, and thus strengthens our already strong correlation with the fragment stability. Other parameters such as carbon precursor pressure, vapor pressure, and feed stock composition have less impact on the chirality of the product, but here we note that the low number of appropriate experimental studies makes it difficult to perform a full evaluation.

Lastly we show that the choice of substrate and catalyst composition can drastically diminish the influence of temperature on the metal particle size and lead to static/frozen metal surfaces that act

as templates for growth of less stable SWNTs, and even lead to metal particle seeds for index specific growth.

References

1. Baughman, R. H., Zakhidov, A. A. & de Heer, W. A. Carbon nanotubes - the route toward applications. *Science* **297,** 787–792 (2002).
2. Cao, Q. *et al.* Arrays of single-walled carbon nanotubes with full surface coverage for high-performance electronics. *Nature Nanotechnology* **8,** 180–186 (2013).
3. Gracia-Espino, E. *et al.* Electrical Transport and Field-Effect Transistors Using Inkjet-Printed SWCNT Films Having Different Functional Side Groups. *ACS Nano* **4,** 3318–3324 (2010).
4. Chae, H. G., Sreekumar, T. V., Uchida, T. & Kumar, S. A comparison of reinforcement efficiency of various types of carbon nanotubes in poly acrylonitrile fiber. *Polymer* **46,** 10925–10935 (2005).
5. Frogley, M. D., Ravich, D. & Wagner, H. D. Mechanical properties of carbon nanoparticle-reinforced elastomers. *Composites Science and Technology* **63,** 1647–1654 (2003).
6. Collins, P. G., Bradley, K., Ishigami, M. & Zettl, A. Extreme oxygen sensitivity of electronic properties of carbon nanotubes. *Science* **287,** 1801–1804 (2000).
7. Cao, Q. & Rogers, J. A. Ultrathin Films of Single-Walled Carbon Nanotubes for Electronics and Sensors: A Review of Fundamental and Applied Aspects. *Advanced Materials* **21,** 29–53 (2009).
8. Mottaghitalab, V., Xi, B. B., Spinks, G. M. & Wallace, G. G. Polyaniline fibres containing single walled carbon nanotubes: Enhanced performance artificial muscles. *Synthetic Metals* **156,** 796–803 (2006).
9. Ding, L. *et al.* Selective Growth of Well-Aligned Semiconducting Single-Walled Carbon Nanotubes. *Nano Letters* **9,** 800–805 (2009).
10. Wang, B. *et al.* (n, m) selectivity of single-walled carbon nanotubes by different carbon precursors on co-mo catalysts. *Journal of the American Chemical Society* **129,** 9014–9019 (2007).
11. Bachilo, S. M. *et al.* Narrow (n, m)-Distribution of Single-Walled Carbon Nanotubes Grown Using a Solid Supported Catalyst. *Journal of the American Chemical Society* **125,** 11186–11187 (2003).
12. Harutyunyan, A. R. *et al.* Preferential Growth of Single-Walled Carbon Nanotubes with Metallic Conductivity. *Science* **326,** 116–120 (2009).
13. Qu, L. T., Du, F. & Dai, L. M. Preferential syntheses of semiconducting vertically aligned single-walled carbon nanotubes for direct use in FETs. *Nano Letters* **8,** 2682–2687 (2008).
14. Fouquet, M. *et al.* Highly chiral-selective growth of single-walled carbon nanotubes with a simple monometallic Co catalyst. *Physical Review B* **85,** 235411 (2012).
15. He, M. *et al.* Selective growth of SWNTs on partially reduced monometallic cobalt catalyst. *Chemical Communications* **47,** 1219–1221 (2011).
16. He, M. *et al.* Predominant (6, 5) Single-Walled Carbon Nanotube Growth on a Copper-Promoted Iron Catalyst. *Journal of the American Chemical Society* **132,** 13994–13996 (2010).
17. He, M., Jiang, H., Kauppinen, E. I. & Lehtonen, J. Diameter and chiral angle distribution dependencies on the carbon precursors in surface-grown single-walled carbon nanotubes. *Nanoscale* **4,** 7394–7398 (2012).
18. He, M. *et al.* Chiral-Selective Growth of Single-Walled Carbon Nanotubes on Lattice-Mismatched Epitaxial Cobalt Nanoparticles. *Scientific Reports* **3,** 1460 (2013).
19. Wang, B., Yang, Y., Li, L. J. & Chen, Y. Effect of different catalyst supports on the (n, m) selective growth of single-walled carbon nanotube from Co-Mo catalyst. *Journal of Materials Science* **44,** 3285–3295 (2009).
20. Barzegar, H. R. *et al.* Simple Dip-Coating Process for the Synthesis of Small Diameter Single-Walled Carbon Nanotubes—Effect of Catalyst Composition and Catalyst Particle Size on Chirality and Diameter. *The Journal of Physical Chemistry C* **116,** 12232–12239 (2012).
21. Wang, H. *et al.* Sulfur doped Co/SiO2 catalysts for chirally selective synthesis of single walled carbon nanotubes. *Chemical Communications* **49,** 2031–2033 (2013).
22. Hersam, M. C. Progress towards monodisperse single-walled carbon nanotubes. *Nature Nanotechnology* **3,** 387–394 (2008).
23. Strano, M. S. *et al.* Electronic structure control of single-walled carbon nanotube functionalization. *Science* **301,** 1519–1522 (2003).
24. Rinzler, A. G. Materials processing - Sorting out carbon nanotube electronics. *Nature Nanotechnology* **1,** 17–18 (2006).
25. Kim, W. J., Usrey, M. L. & Strano, M. S. Selective functionalization and free solution electrophoresis of single-walled carbon nanotubes: Separate enrichment of metallic and semiconducting SWNT. *Chemistry of Materials* **19,** 1571–1576 (2007).
26. Chattopadhyay, D., Galeska, I. & Papadimitrakopoulos, F. A route for bulk separation of semiconducting from metallic single-wall carbon nanotubes. *Journal of the American Chemical Society* **125,** 3370–3375 (2003).
27. Kim, S. N., Luo, Z. T. & Papadimitrakopoulos, F. Diameter and metallicity dependent redox influences on the separation of single-wall carbon nanotubes. *Nano Letters* **5,** 2500–2504 (2005).
28. Balasubramanian, K., Sordan, R., Burghard, M. & Kern, K. A selective electrochemical approach to carbon nanotube field-effect transistors. *Nano Letters* **4,** 827–830 (2004).
29. Arnold, M. S., Green, A. A., Hulvat, J. F., Stupp, S. I. & Hersam, M. C. Sorting carbon nanotubes by electronic structure using density differentiation. *Nature Nanotechnology* **1,** 60–65 (2006).
30. Khripin, C. Y., Fagan, J. A. & Zheng, M. Spontaneous Partition of Carbon Nanotubes in Polymer-Modified Aqueous Phases. *Journal of the American Chemical Society* **135,** 6822–6825 (2013).
31. Ao, G. Y., Khripin, C. Y. & Zheng, M. DNA-Controlled Partition of Carbon Nanotubes in Polymer Aqueous Two-Phase Systems. *Journal of the American Chemical Society* **136,** 10383–10392 (2014).
32. Barzegar, H. R., Gracia-Espino, E., Sharifi, T., Nitze, F. & Wagberg, T. Nitrogen Doping Mechanism in Small Diameter Single-Walled Carbon Nanotubes: Impact on Electronic Properties and Growth Selectivity. *Journal of Physical Chemistry C* **117,** 25805–25816 (2013).
33. Krstic, V. *et al.* Indirect Magnetic Coupling in Light-Element-Doped Single-Walled Carbon Nanotubes. *ACS Nano* **4,** 5081–5086 (2010).
34. Lee, R. S., Kim, H. J., Fischer, J. E., Thess, A. & Smalley, R. E. Conductivity enhancement in single-walled carbon nanotube bundles doped with K and Br. *Nature* **388,** 255–257 (1997).
35. Rao, C. N. R., Satishkumar, B. C., Govindaraj, A. & Nath, M. Nanotubes. *Chemphyschem* **2,** 78–105 (2001).
36. Takenobu, T. *et al.* Stable and controlled amphoteric doping by encapsulation of organic molecules inside carbon nanotubes. *Nature Materials* **2,** 683–688 (2003).
37. Avouris, P. Carbon nanotube electronics. *Chemical Physics* **281,** 429–445 (2002).
38. Peng, S. & Cho, K. J. Chemical control of nanotube electronics. *Nanotechnology* **11,** 57–60 (2000).

39. Ehli, C. *et al.* Manipulating single-wall carbon nanotubes by chemical doping and charge transfer with perylene dyes. *Nature Chemistry* **1,** 243–249 (2009).
40. Kazaoui, S., Minami, N., Matsuda, N., Kataura, H. & Achiba, Y. Electrochemical tuning of electronic states in single-wall carbon nanotubes studied by *in situ* absorption spectroscopy and ac resistance. *Applied Physics Letters* **78,** 3433–3435 (2001).
41. McGuire, K. *et al.* Synthesis and Raman characterization of boron-doped single-walled carbon nanotubes. *Carbon* **43,** 219–227 (2005).
42. Terrones, M. Carbon nanotubes: synthesis and properties, electronic devices and other emerging applications. *International Materials Reviews* **49,** 325–377 (2004).
43. Wagner, R. S. & Ellis, W. C. Vapor-Liquid-Solid Mechanism of Single Crystal Growth (New Method Growth Catalysis from Impurity Whisker Epitaxial + Large Crystals Si E). *Applied Physics Letters* **4,** 89–90 (1964).
44. Baker, R. T. K., Barber, M. A., Waite, R. J., Harris, P. S. & Feates, F. S. Nucleation and Growth of Carbon Deposits from Nickel Catalyzed Decomposition of Acetylene. *Journal of Catalysis* **26,** 51–62 (1972).
45. Rodriguez-Manzo, J. A. *et al. In situ* nucleation of carbon nanotubes by the injection of carbon atoms into metal particles. *Nature Nanotechnology* **2,** 307–311 (2007).
46. Ding, F. *et al.* The importance of strong carbon-metal adhesion for catalytic nucleation of single-walled carbon nanotubes. *Nano Letters* **8,** 463–468 (2008).
47. Larsson, P. *et al.* Calculating carbon nanotube-catalyst adhesion strengths. *Physical Review B* **75,** 115419 (2007).
48. Robertson, J. Heterogeneous catalysis model of growth mechanisms of carbon nanotubes, graphene and silicon nanowires. *Journal of Materials Chemistry* **22,** 19858–19862 (2012).
49. Silvearv, F., Larsson, P., Jones, S. L. T., Ahuja, R. & Larsson, J. A. Establishing the most favorable metal-carbon bond strength for carbon nanotube catalysts. *Journal of Materials Chemistry C* **3,** 3422–3427 (2015).
50. Li, Z. *et al.* Copper/molybdenum nanocomposite particles as catalysts for the growth of bamboo-structured carbon nanotubes. *Journal of Physical Chemistry C* **112,** 12201–12206 (2008).
51. O'Byrne, J. P. *et al.* Growth of Carbon Nanotubes from Heterometallic Palladium and Copper Catalysts. *Journal of Physical Chemistry C* **114,** 8115–8119 (2010).
52. Wang, H. *et al.* Selective Synthesis of (9, 8) Single Walled Carbon Nanotubes on Cobalt Incorporated TUD-1 Catalysts. *Journal of the American Chemical Society* **132,** 16747–16749 (2010).
53. Chiang, W.-H. & Mohan Sankaran, R. Linking catalyst composition to chirality distributions of as-grown single-walled carbon nanotubes by tuning NixFe1-x nanoparticles. *Nature Materials* **8,** 882–886 (2009).
54. Wang, H. *et al.* Chiral-Selective CoSO4/SiO2 Catalyst for (9,8) Single-Walled Carbon Nanotube Growth. *ACS Nano* **7,** 614–626 (2012).
55. Ago, H. *et al.* CVD Growth of Single-Walled Carbon Nanotubes with Narrow Diameter Distribution over Fe/MgO Catalyst and Their Fluorescence Spectroscopy. *The Journal of Physical Chemistry B* **109,** 10035–10041 (2005).
56. Lolli, G. *et al.* Tailoring (n, m) Structure of Single-Walled Carbon Nanotubes by Modifying Reaction Conditions and the Nature of the Support of CoMo Catalysts. *The Journal of Physical Chemistry B* **110,** 2108–2115 (2006).
57. Wang, B. *et al.* Pressure-Induced Single-Walled Carbon Nanotube (n, m) Selectivity on Co−Mo Catalysts. *The Journal of Physical Chemistry C* **111,** 14612–14616 (2007).
58. Baran, J. D., Kolodziejczyk, W., Larsson, P., Ahuja, R. & Larsson, J. A. On the stability of single-walled carbon nanotubes and their binding strengths. *Theoretical Chemistry Accounts* **131,** 1270 (2012).
59. Li, Y. G., Ahuja, R. & Larsson, J. A. Communication: Origin of the difference between carbon nanotube armchair and zigzag ends. *Journal Of Chemical Physics* **140,** 091102 (2014).
60. Reich, S., Li, L. & Robertson, J. Control the chirality of carbon nanotubes by epitaxial growth. *Chemical Physics Letters* **421,** 469–472 (2006).
61. Dutta, D., Chiang, W. H., Sankaran, R. M. & Bhethanabotla, V. R. Epitaxial nucleation model for chiral-selective growth of single-walled carbon nanotubes on bimetallic catalyst surfaces. *Carbon* **50,** 3766–3773 (2012).
62. Reich, S., Li, L. & Robertson, J. Structure and formation energy of carbon nanotube caps. *Physical Review B* **72,** 165423 (2005).
63. Penev, E. S., Artyukhov, V. I. & Yakobson, B. I. Extensive Energy Landscape Sampling of Nanotube End-Caps Reveals No Chiral-Angle Bias for Their Nucleation. *Acs Nano* **8,** 1899–1906 (2014).
64. Artyukhov, V. I., Penev, E. S. & Yakobson, B. I. Why nanotubes grow chiral. *Nature Communications* **5,** 4892 (2014).
65. Ding, F., Harutyunyan, A. R. & Yakobson, B. I. Dislocation theory of chirality-controlled nanotube growth. *Proceedings of the National Academy of Sciences of the United States of America* **106,** 2506–2509 (2009).
66. Bachilo, S. M. *et al.* Structure-assigned optical spectra of single-walled carbon nanotubes. *Science* **298,** 2361–2366 (2002).
67. Dresselhaus, M. S., Dresselhaus, G., Saito, R. & Jorio, A. Raman spectroscopy of carbon nanotubes. *Physics Reports-Review Section of Physics Letters* **409,** 47–99 (2005).
68. Pimenta, M. A. *et al.* Resonant Raman effect in single-wall carbon nanotubes. *Journal of Materials Research* **13,** 2396–2404 (1998).
69. Yang, F. *et al.* Chirality-specific growth of single-walled carbon nanotubes on solid alloy catalysts. *Nature* **510,** 522–524 (2014).
70. Jorio, A. *et al.* Quantifying carbon-nanotube species with resonance Raman scattering. *Physical Review B* **72,** 075207 (2005).
71. Kresse, G. & Furthmuller, J. Efficient iterative schemes for ab initio total-energy calculations using a plane-wave basis set. *Physical Review B* **54,** 11169–11186 (1996).
72. Blochl, P. E. Projector Augmented-Wave Method. *Physical Review B* **50,** 17953–17979 (1994).
73. Perdew, J. P., Burke, K. & Ernzerhof, M. Generalized gradient approximation made simple. *Physical Review Letters* **77,** 3865–3868 (1996).
74. Mole, S. J., Zhou, X. F. & Liu, R. F. Density functional theory (DFT) study of enthalpy of formation. 1. Consistency of DFT energies and atom equivalents for converting DFT energies into enthalpies of formation. *Journal of Physical Chemistry* **100,** 14665–14671 (1996).
75. Hod, O., Peralta, J. E. & Scuseria, G. E. Edge effects in finite elongated graphene nanoribbons. *Physical Review B* **76,** 233401 (2007).
76. Hod, O. & Scuseria, G. E. Electromechanical Properties of Suspended Graphene Nanoribbons. *Nano Letters* **9,** 2619–2622 (2009).
77. Rochefort, A., Salahub, D. R. & Avouris, P. Effects of finite length on the electronic structure of carbon nanotubes. *Journal of Physical Chemistry B* **103,** 641–646 (1999).
78. Fouquet, M. *et al.* Effect of Catalyst Pretreatment on Chirality-Selective Growth of Single-Walled Carbon Nanotubes. *The Journal of Physical Chemistry C* **118,** 5773–5781 (2014).
79. He, M. *et al.* Chiral-selective growth of single-walled carbon nanotubes on stainless steel wires. *Carbon* **50,** 4294–4297 (2012).
80. Li, X. *et al.* Selective Synthesis Combined with Chemical Separation of Single-Walled Carbon Nanotubes for Chirality Selection. *Journal of the American Chemical Society* **129,** 15770–15771 (2007).
81. Li, N., Wang, X., Ren, F., Haller, G. L. & Pfefferle, L. D. Diameter Tuning of Single-Walled Carbon Nanotubes with Reaction Temperature Using a Co Monometallic Catalyst. *The Journal of Physical Chemistry C* **113,** 10070–10078 (2009).
82. Miyauchi, Y., Chiashi, S., Murakami, Y., Hayashida, Y. & Maruyama, S. Fluorescence spectroscopy of single-walled carbon nanotubes synthesized from alcohol. *Chemical Physics Letters* **387,** 198–203 (2004).

83. Volotskova, O. *et al.* Tailored Distribution of Single-Wall Carbon Nanotubes from Arc Plasma Synthesis Using Magnetic Fields. *ACS Nano* **4,** 5187–5192 (2010).
84. Wang, B. *et al.* (n, m) Selectivity of Single-Walled Carbon Nanotubes by Different Carbon Precursors on Co−Mo Catalysts. *Journal of the American Chemical Society* **129,** 9014–9019 (2007).
85. Wei, L. *et al.* Narrow-chirality distributed single-walled carbon nanotube synthesis by remote plasma enhanced ethanol deposition on cobalt incorporated MCM-41 catalyst. *Carbon* **66,** 134–143 (2014).
86. Zoican Loebick, C. *et al.* Selective Synthesis of Subnanometer Diameter Semiconducting Single-Walled Carbon Nanotubes. *Journal of the American Chemical Society* **132,** 11125–11131 (2010).
87. Maruyama, T., Mizutani, Y., Naritsuka, S. & Iijima, S. Single-Walled Carbon Nanotube Growth in High Vacuum Using Pt Catalyst in Alcohol Gas Source Method. *Materials Express* **1,** 267–272 (2011).
88. Zhu, Z., Jiang, H., Susi, T., Nasibulin, A. G. & Kauppinen, E. I. The Use of NH3 to Promote the Production of Large-Diameter Single-Walled Carbon Nanotubes with a Narrow (n, m) Distribution. *Journal of the American Chemical Society* **133,** 1224–1227 (2010).
89. Sanchez-Valencia, J. R. *et al.* Controlled synthesis of single-chirality carbon nanotubes. *Nature* **512,** 61–64 (2014).
90. Jin-Ju, K., Byeong-Joo, L., Seung-Hwan, L. & Goo-Hwan, J. Size engineering of metal nanoparticles to diameter-specified growth of single-walled carbon nanotubes with horizontal alignment on quartz. *Nanotechnology* **23,** 105607 (2012).
91. Nasibulin, A. G., Pikhitsa, P. V., Jiang, H. & Kauppinen, E. I. Correlation between catalyst particle and single-walled carbon nanotube diameters. *Carbon* **43,** 2251–2257 (2005).
92. Robertson, D. H., Brenner, D. W. & Mintmire, J. W. Energetics of Nanoscale Graphitic Tubules. *Physical Review B* **45,** 12592–12595 (1992).
93. Sawada, S. & Hamada, N. Energetics of Carbon Nanotubes. *Solid State Communications* **83,** 917–919 (1992).
94. Simpson, J. R., Fagan, J. A., Becker, M. L., Hobbie, E. K. & Hight Walker, A. R. The effect of dispersant on defects in length-separated single-wall carbon nanotubes measured by Raman spectroscopy. *Carbon* **47,** 3238–3241 (2009).
95. Borjesson, A. & Bolton, K. Modeling of Ostwald Ripening of Metal Clusters Attached to Carbon Nanotubes. *Journal of Physical Chemistry C* **115,** 24454–24462 (2011).
96. Borjesson, A. & Bolton, K. First Principles Studies of the Effect of Ostwald Ripening on Carbon Nanotube Chirality Distributions. *ACS Nano* **5,** 771–779 (2011).
97. Kim, S. M. *et al.* Evolution in Catalyst Morphology Leads to Carbon Nanotube Growth Termination. *Journal of Physical Chemistry Letters* **1,** 918–922 (2010).
98. Yang, Z. J. *et al.* Mesoporous CeO2 Hollow Spheres Prepared by Ostwald Ripening and Their Environmental Applications. *European Journal of Inorganic Chemistry* **2010,** 3354–3359 (2010).
99. Picher, M., Anglaret, E., Arenal, R. & Jourdain, V. Processes Controlling the Diameter Distribution of Single-Walled Carbon Nanotubes during Catalytic Chemical Vapor Deposition. *Acs Nano* **5,** 2118–2125 (2011).
100. Iglesia, E., Baumgartner, J. E. & Price, G. L. Kinetic coupling and hydrogen surface fugacities in heterogeneous catalysis: I. Alkane reactions on Te/NaX, H-ZSM5, and Ga/H-ZSM5. *Journal of Catalysis* **134,** 549–571 (1992).
101. Haller, G. L. & Resasco, D. E. in *Advances in Catalysis* Vol. Volume 36 (eds Herman Pines D.D. Eley & B. Weisz Paul) 173–235. (Academic Press, 1989).
102. Smalley, R. E. *et al.* Single Wall Carbon Nanotube Amplification: En Route to a Type-Specific Growth Mechanism. *Journal of the American Chemical Society* **128,** 15824–15829 (2006).
103. Yang, F. *et al.* Growing Zigzag (16, 0) Carbon Nanotubes with Structure-Defined Catalysts. *Journal of the American Chemical Society* **137,** 8688–8691 (2015).
104. Kawase, T. & Kurata, H. Ball-, bowl-, and belt-shaped conjugated systems and their complexing abilities: Exploration of the concave-convex pi-pi interaction. *Chemical Reviews* **106,** 5250–5273 (2006).

Acknowledgements

Author Contributions

Conceptual idea by J.A.L. following discussion with T.W. and A.R. H.R.B. compiled the table of all experiments with proper analysis of the SWNT product in collaboration with T.W., which was reviewed by all. H.R.B. and T.W. prepared Fig. 3. D.H. performed the DFT simulations and prepared Fig. 1 and 2 with J.A.L. and contributions from all. J.A.L., T.W. and A.R. authored the main manuscript, with progression from reviews by all. H.R.B. authored the growth parameter discussion section with contributions from all.

Additional Information

Supplementary information accompanies this paper at http://www.nature.com/srep

Competing financial interests: The authors declare no competing financial interests.

How to cite this article: Hedman, D. *et al.* On the Stability and Abundance of Single Walled Carbon Nanotubes. *Sci. Rep.* **5,** 16850; doi: 10.1038/srep16850 (2015).